PHYSICAL REVIEW B VOLUME 47, NUMBER 10 1 MARCH 1993-II

Mössbauer study of the high-temperature phase of Co-substituted magnetites, $Co_xFe_{3-x}O_4$. I. $x \leq 0.04$

E. De Grave, R. M. Persoons,* R. E. Vandenberghe, and P. M. A. de Bakker
Laboratory of Magnetism, University of Gent, Proeftuinstraat 86, B-9000 Gent, Belgium

(Received 19 February 1992; revised manuscript received 21 July 1992)

Six Co-substituted magnetites $Co_xFe_{3-x}O_4$, with $x \leq 0.04$ have been studied by ^{57}Fe Mössbauer spectroscopy at temperatures T between their respective Verwey transition and ≈900 K. The Curie temperature T_C decreases from 868 K for $x=0$ to 859 K for $x=0.03$. All spectra were decomposed into tetrahedral (A-site) and octahedral (B-site) components. The obtained results are consistent with the fact that at low temperatures above the Verwey transition, the spins lie along a domain's [100] axis, but flip to a [111] axis at a temperature strongly increasing with increasing x. The temperature variations of the hyperfine parameters (center shift δ, quadrupole shift ε_Q, magnetic hyperfine field H_{hf} and dipolar field H_{dip}) have been determined. The δ and H_{hf} values for the octahedral Fe are consistent with the well-known fast electron exchange between the involved Fe^{2+} and Fe^{3+} species. From the temperature dependence of the B-site linewidth it is concluded that the nature of the exchange process at relatively low temperatures, depending on x, is different from that at higher temperatures. The ε_Q vs T and H_{dip} vs T curves for the B sites of the $x=0$, 0.005, and 0.01 samples (both mentioned parameters for the A sites are zero) were interpreted on the basis of a common crystalline-field model, yielding, as argued, unrealistic values for certain involved physical quantities. The behavior of the center shifts implies a slight temperature variation for the intrinsic isomer shift. Unlike the A-site hyperfine fields, the temperature dependence of the B-site fields could not be reproduced adequately by the usual formulas based on Heisenberg-type exchange. Instead, a non-localized-electron model led to an excellent description of the experimental curves. The bandwidth, which appears in that model, turned out to be high (0.82 eV for $x=0$ at 300 K) and is suggested to be responsible for the failure of the crystalline-field model to explain the temperature variation of $e^2qQ/2$ and H_{dip}. For all compositions ε_Q and H_{dip} at selected temperatures have also been determined from spectra recorded in external magnetic fields. These spectra further indicate that a field-induced contribution to the total hyperfine field on the B sites (not on A sites) is to be taken into account. Its origin is discussed briefly.

I. INTRODUCTION

Magnetite, Fe_3O_4 is a binary spinel oxide with one Fe^{3+} ion per formula unit on the tetrahedral site (A site) and one Fe^{3+} and one Fe^{2+} ion on the octahedral sites (B sites). The compound is particularly interesting because of its Verwey transition (VT) which, for stoichiometric magnetite, takes place at $T_V=122$ K.[1,2] Below T_V the structure is monoclinic,[3] whereas above T_V it is cubic with lattice parameter $a=0.8397$ nm.[4] The crystallographic transition is accompanied by an electronic transition: in the high-temperature phase, the sixth $3d$ electron is not localized, resulting in a high electric conductivity.[2]

Both the low- and the high-temperature phases of magnetite have been studied very intensively by numerous techniques, not the least using Mössbauer spectroscopy, already dating back to 1961.[5] The transition is clearly reflected in the Mössbauer spectra. However, up till now an adequate model for the interpretation of the spectra recorded below T_V has not been found yet, suggesting that the magnetic and electronic structure of the low-temperature phase is extremely complicated. Dormann, Djega-Mariadassou, and Brabers[6] considered five distinct sextet components with different hyperfine parameters and attributed these to different charge states for the iron between and including bivalent and trivalent ones. One of the present authors recently applied that model,[7] however, came to the conclusion that significant discrepancies between experimental and calculated spectra still remain.

In contrast, the spectra characterizing the high-temperature (HT) phase are much simpler and basically consist of two sextet components with a nearly 1:2 area ratio and arising, respectively, from tetrahedral and octahedral iron. The room-temperature (RT) hyperfine parameters, as reported in the literature,[8-14] to some extent are scattered within not so narrow intervals: 480–498 kOe and 450–463 kOe for the A- and B-site hyperfine field, $H_{\mathrm{hf},A}$ and $H_{\mathrm{hf},B}$, respectively, and 0.27–0.32 mm/s and 0.60–0.69 mm/s for the respective center shifts δ_A and δ_B vs metallic iron. All authors agree that the quadrupole shift ϵ_Q as measured from the magnetic spectra is zero within the experimental error limits for both sites.

More recently, several groups recognized the fact that the HT B-site component actually consists of two distinct subspectra as a result of two different orientations of the electric field gradient's (EFG's) principal axis with respect to the direction of the hyperfine field.[15-19] This feature will be presented in more detail in the section on data analysis.

The B-site hyperfine parameters are neither typical for Fe^{3+} nor for Fe^{2+}. This led to the suggestion that the sixth $3d$ electron jumps between adjacent Fe^{3+} and Fe^{2+} ions along the [110] B-site chains with a frequency which is considerably higher than the inverse of the Mössbauer measuring time. As a consequence, the Mössbauer effect sees an average valency state, usually denoted as $Fe^{2.5+}$.

The exact nature of the electron diffusion process is long since the subject of vivid debate, not only among Mössbauer spectroscopists. Several authors attempted to obtain some insight into the process by studying the Mössbauer spectra of substituted magnetites, $M_xFe_{3-x}O_4$, with M a transition metal. Both A- (Refs. 20–22) and B-site (Refs. 23–28) substitutions have been considered, and some authors explained their findings by a pairwise hopping model, while others preferred an electron exchange via a conduction band extending throughout the entire B-site sublattice. In a recent paper, Ihle and Lorenz[29] argued that the conductivity of Fe_3O_4 above the VT results from a superposition of small-polaron band and small-polaron hopping conduction, the former one being the dominant mechanism below RT.

In this first of two companion papers, the authors present their results of an extensive Mössbauer study on Co-substituted magnetites, $Co_xFe_{3-x}O_4$, with emphasis on the small substitutions, i.e., x up to 0.04, for which, as will be shown, the electron exchange is the dominant feature determining the spectra at temperatures above the VT. The second paper will be devoted to higher x values ($x \geq 0.1$). In this range, an additional complication arises from the chemical disorder as a result of the presence of a substantial amount of Co in the magnetite lattice.

II. EXPERIMENTAL

Five different compositions of the $Co_xFe_{3-x}O_4$ solid-solution series have been considered for this part of the study. They had x values of 0.005, 0.01, 0.02, 0.03, and 0.04. They were originally single crystals of which a small part was removed for the Mössbauer absorbers.

The crushed parts were hand ground and the powders were afterwards annealed at 600 °C in a vacuum furnace in order to minimize the number of defects possibly introduced by the grinding. All absorbers had a thickness of 10 mg Fe/cm^2. For completeness, a supposedly pure, commercial polycrystalline Fe_3O_4 sample was included as well.

Transmission spectra were recorded in 1024 channels using time-mode spectrometers with triangular reference signal. The source was ^{57}Co in a Rh matrix, but all isomer-shift values quoted hereafter are referenced with respect to metallic iron. All spectra were run until an off-resonance count rate of at least 10^6 (unfolded spectrum) was reached. The spectrometers were calibrated either interferometrically or using the spectra of a calibrated hematite absorber. These spectra were recorded simultaneously using a second Rh source and counting system at the opposite end of the transducer. Typically the increment of one channel was 0.04 mm/s and the instrumental width better than 0.22 mm/s. Deviations from linearity of the velocity scale were less than 0.1%.

In the range 4.2–500 K, the temperature T was varied using a commercial flow-cryostate-furnace combination with a proportional-integral-derivative (PID) temperature controller providing a stability of 0.2 K for the indicated temperature over the accumulation period of 12–24 h. Higher temperatures up to 900 K for selected compositions ($x = 0, 0.01, 0.03$) were obtained in a commercial vacuum furnace with similar control and performance. For all compositions the temperature range was scanned in steps of 20–30°, yielding a total number of spectra of close to 200, and a huge amount of numerical data which will be made available on request.

Several spectra were recorded with the absorber in a longitudinal external magnetic field with strength ranging between 10 and 60 kOe. In this arrangement the temperature could be varied between 4.2 and 300 K. The source was always at room temperature.

III. INTERPRETATION OF THE SPECTRA

Most spectra in the low-substitution range and below the respective Curie temperature T_C were fitted using symmetrical, Lorentzian-shaped sextet components of which the hyperfine field, the quadrupole shift, and center shift, and two width parameters for each sextet were adjusted by nonlinear least-squares fitting. The two width parameters were Γ and $\Delta\Gamma$ which determine the width of the six lines as $\Gamma_1 = \Gamma_6 = \Gamma + 2\Delta\Gamma$, $\Gamma_2 = \Gamma_5 = \Gamma + \Delta\Gamma$, and $\Gamma_3 = \Gamma_4 = \Gamma$. The broadening parameter $\Delta\Gamma$ is introduced in order to account for any slight hyperfine-field distribution resulting from, e.g., a nonunique structural surrounding for the probe nuclei. It turned out that at $T \leq 0.9T_C$ its value was always reasonably small (typically 0.01 mm/s at RT for the A sites). The background and three area parameters per component were fitted by a linear least-squares routine. Unless otherwise stated, no other restrictions on the Mössbauer parameters were imposed in the fitting.

For T exceeding ≈ 140 K, the B-site spins, and hence the hyperfine field, in nonsubstituted magnetite are along a domain's [111] axis.[30] Due to the trigonal local symmetry on the B sites, which is common for spinel compounds,[31] the EFG's main axis is along a local [111] axis. This means that the angle θ between $H_{\mathrm{hf},B}$ and the EFG takes on two values, i.e., 0° and 70.5° in a ratio 1:3, respectively. As a result of the expression

$$\epsilon_Q = \frac{e^2qQ}{4}\,\frac{3\cos^2\theta - 1}{2}\ , \tag{1}$$

with $e^2qQ/2 = \Delta E_Q$ the nonzero quadrupole splitting as would be observed if the material were paramagnetic, two different B-site components with different ϵ_Q values are generated, i.e., $\epsilon_{Q1} = \Delta E_Q/2$ and $\epsilon_{Q2} = -\Delta E_Q/6$, with ratio 1:3, respectively. Moreover, the two subpatterns also exhibit a different hyperfine field due to a dipolar shift ϵ_{dip} which shows a similar θ dependence:

$$\epsilon_{\mathrm{dip}} = H_{\mathrm{dip}}\frac{3\cos^2\theta - 1}{2}\ , \tag{2}$$

with H_{dip} the dipolar-field contribution. This leads to shifts $\epsilon_{\mathrm{dip1}} = H_{\mathrm{dip}}$ and $\epsilon_{\mathrm{dip2}} = -H_{\mathrm{dip}}/3$. This means that the two distinct B sites have fields $H_{\mathrm{hf},B1}=H_{\mathrm{hf},B}+H_{\mathrm{dip}}$ and $H_{\mathrm{hf},B2}=H_{\mathrm{hf},B}-H_{\mathrm{dip}}/3$, respectively, in which $H_{\mathrm{hf},B}$ contains the Fermi-contact term, reduced by covalency, and any other additional contributions other than the dipolar one.

In the temperature range between T_V and ≈ 130 K, the hyperfine field is along a domain's [100] axis and $\theta=54.7°$ for all B sites. Expressions (1) and (2) then yield $\epsilon_Q=0$ and $\epsilon_{\mathrm{dip}}=0$. Finally, in the range $\approx 130-140$ K, the easy axis is [110], leading to angles of 90° and 35.3° in a 1:1 ratio, and shifts of $\pm\Delta E_Q/4$ and $\pm H_{\mathrm{dip}}/2$. As for the A sites, the local symmetry is cubic. Hence, there is no EFG and consequently only one Mössbauer component.

According to Bickford, Pappis, and Stull,[30] and in agreement with the magnetostriction experiments of Leyman,[32] for Co substitutions $x \geq 0.005$ an intermediate temperature range with spins along [110] could not be detected and the [100]-to-[111] transition drastically shifts to higher T on increasing x: 200, 275, and 390 K for $x=0.005$, 0.01, and 0.02, respectively. No data are available for higher substitutions. These T values are found to be in line with the present Mössbauer results, although it was not attempted in this study to accurately determine these, nor to search for the existence of an intermediate spin orientation.

In view of the strong overlap of the absorption lines, the spectra of a selected composition were additionally analyzed with the transmission integral. The evaluated parameter values were not significantly different from those obtained from the Lorentz approximation.

In an external field $H_{\mathrm{ext}} \geq 20$ kOe, the $\Delta m_I=0$ transitions for the involved $\mathrm{Co}_x\mathrm{Fe}_{3-x}\mathrm{O}_4$ samples are observed to be absent in both A- and B-site components, meaning that the spins are aligned along $\mathbf{H}_{\mathrm{ext}}$. The spin direction is therefore random with respect to the B-site EFG's principal axis, and due to the θ dependence of the dipolar contribution [expression (2)], the B-site hyperfine field becomes anisotropic. As a result, the line shape of the octahedral subpattern in the applied-field Mössbauer spectra (AFMS) is no longer symmetrical.[33,34] If the EFG's asymmetry parameter η equals zero, which is presumably true for the involved magnetites, then each absorption line S_j ($j=1,\ldots,6$) as a function of the source velocity v has to be written as

$$S_j(v)=\frac{1}{4\rho_j[2\mu_j(v)-1]}\left\{\sigma_j(v)\ln\left[\frac{1+\tau_j(v)-\mu_j(v)}{1-\tau_j(v)-\mu_j(v)}\right]+\tau_j(v)\left[\pi+\mathrm{sgn}[\mu_j(v)]\left[\pi-2\left|\tan^{-1}\frac{\sigma_j(v)}{\mu_j(v)}\right|\right]\right]\right\}, \tag{3}$$

with

$$\mu_j(v)=\tfrac{1}{2}\{1-[\omega_j^2(v)+1]^{1/2}/\rho_j\}, \tag{4}$$

$$\sigma_j(v)=[\tfrac{1}{2}-\mu_j(v)+\omega_j(v)/2\rho_j]^{1/2}, \tag{5}$$

$$\tau_j(v)=-1/2\sigma_j(v)\rho_j, \tag{6}$$

$$\omega_j(v)=\left[v-\delta-\alpha_j\left[H_{\mathrm{eff}}-\frac{H_{\mathrm{dip}}}{2}\right]+\beta_j\frac{e^2qQ}{4}\right]\frac{2}{\Gamma_j}, \tag{7}$$

$$\rho_j=-\frac{3}{2}\left[\beta_j\frac{e^2qQ}{4}+\alpha_jH_{\mathrm{dip}}\right]\frac{2}{\Gamma_j}. \tag{8}$$

$\beta_1=\beta_6=1$, $\beta_2=\beta_3=\beta_4=\beta_5=-1$, $\alpha_1=\alpha_6=0.016\,125$, $\alpha_2=\alpha_5=0.009\,336$, $\alpha_3=\alpha_4=0.002\,546$, all in mm $(s\,\mathrm{kOe})^{-1}$.

A fitting routine based on these seemingly complicated expressions and using a combination of nonlinear and linear least-squares iterations similar to that used for the zero-field spectra (ZFMS), was developed by one of the authors to interpret the AFMS, hereby assuming that both B-site components had equal width parameters. There is only one additional parameter to be adjusted, at least for the B-site component, i.e., H_{dip}. After some experience was gained, it was realized that fitting e^2qQ and H_{dip}, both quantities being small and strongly interfering, very often led to unrealistic results and it was therefore decided to fix e^2qQ at its value obtained from the ZFMS.

IV. RESULTS

A minor part of the results of this Mössbauer study on $\mathrm{Co}_x\mathrm{Fe}_{3-x}\mathrm{O}_4$ with $x \leq 0.04$ has been presented in previous communications from this laboratory. The first one[35] concerned ZFMS and AFMS at RT from which it was concluded that the Co ions enter the octahedral sites. A peculiar feature was observed in the $x=0.04$ AFMS in which an additional, but weak ($\approx 3\%$ of the total absorption) component was observed. On the basis of its hyperfine parameters, this component had to be attributed to octahedral Fe^{3+} and it was suggested that, due to the Co substitution, some of the Fe^{3+} ions do not pair with adjacent Fe^{2+} and are therefore not involved in the electron exchange process. This suggestion has been confirmed by later experiments on the highly substituted magnetites and will be discussed in the forthcoming paper.

In a subsequent paper,[36] the experiments aimed to determine T_V as a function of x have been reported. The VT was found to be very sharp and shifted from 122 K for $x=0.005$ to 97 K for $x=0.04$, in excellent agreement with Leyman's magnetostriction results.[32] The value found for the $x=0$ ($T_V=116$ K) was clearly not in line with those of the substituted samples, indicating that the commercial sample is of poorer quality as far as its stoichiometry is concerned.

Finally, the third communication was devoted to the dipolar-field effects in the samples $x=0$, 0.005, and 0.01.[37] Following the claim of Boekema[38] with respect to nonsubstituted magnetite, it was suggested in the paper that the magnitude of the dipolar field had a maximum at around 250 K. More recent, and more precise experiments reported in this paper, however, have questioned this suggestion.

Experimental and calculated Mössbauer spectra for $x=0.03$ at some selected temperatures are shown in Fig. 1. At a given temperature all samples had very similar spectral features and cannot be distinguished visually. The Mössbauer parameters for $x=0$ and again for selected temperatures are listed in Table I. The quadrupole shift $\epsilon_{Q,A}$ for the A-site ferric ions has not been included since in all cases it turned out to be zero within experimental error limits. The quantity F_i in Table I is the relative spectral area corresponding to site i and the indicated linewidths refer to the outermost lines (1 and 6). The errors are 1 kOe for H_{hf}, 0.005 mm/s for δ, 0.01 mm/s for $\Gamma^{1,6}$, 1% for F_A and 2% for F_B, 0.5 kOe for H_{dip}, and 0.01 mm/s for ϵ_Q.

As mentioned earlier, $H_{\mathrm{hf},B}$ is the sum of all contributions to the hyperfine field (Fermi-contact field, covalency reduction, and any other possible contributions), except the dipolar one when present. It should be noted that for $T=135$ K, the ratio $F_{B1}:F_{B2}$ was fixed at 1:1 (spins along [110]) whereas for all other T values up to 500 K the ratio was adjusted. It is clear that the 1:3 ideal ratio is closely approximated by the fittings. Also, the signs and the relative magnitudes of the fitted B-site ϵ_Q values are in reasonable agreement with the theoretical considerations outlined in the previous section. Similar results were obtained for $x=0.005$ and $x=0.01$. At high temperatures depending on x, the dipolar field has become too small to enable decomposition of the B-site component. Similarly, for $x=0.02$ and on, the [100]-to-[111] spin-flip transitions are expected to take place at such high T values that the dipolar effects are no longer observable.

The magnetic order-disorder transition, measured carefully for $x=0$, 0.01, and 0.03, is very sharp for the two latter ones (less than 10°), but much broader ($\approx 25°$) for the $x=0$ sample, again pointing at its poorer stoichiometry. The Curie temperature T_C for the three samples was found to be 868±4, 861±2, and 859±1 K, respectively. Håggström *et al.*[17] reported a value of 840 K and Evans[39] 855 K both from their Mössbauer measurements on Fe_3O_4, whereas Riste and Tenzer[40] found 869 K from neutron diffraction. As commented by Håggström *et al.*, this wide scatter of T_c values probably reflects the different stoichiometries of the various Fe_3O_4 samples.

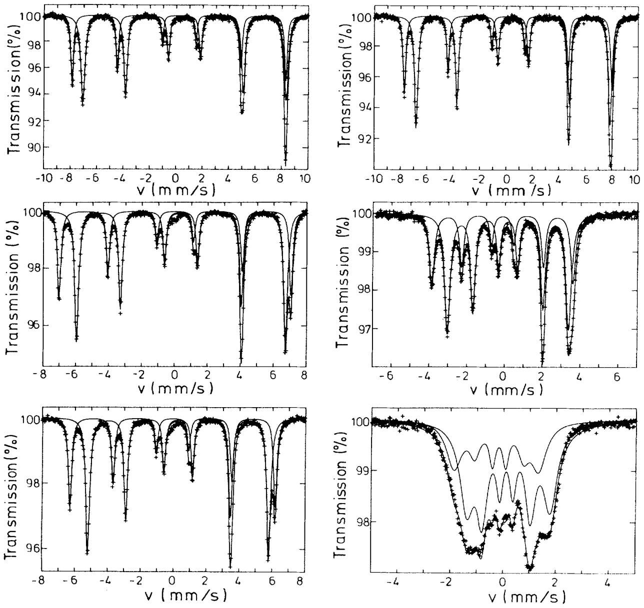

FIG. 1. Selection of Mössbauer spectra of $Co_{0.03}Fe_{2.97}O_4$ at different temperatures. The full lines are the A- and B-site Lorentzian-shaped sextets and their sum fitted to the experimental data. The largest hyperfine field arises from the tetrahedral ferric ions.

For temperatures exceeding T_C, the spectra are best described by the sum of an A-site singlet and a B-site

TABLE I. Mössbauer parameters at some selected temperatures for the A- and B-site iron ions in the nonsubstituted Fe_3O_4 sample. For $T \geq 588$ K, only one B-site component can be resolved from the spectra and the dipolar field H_{dip} cannot be determined. The δ values are referenced against metallic Fe at room temperature.

T (K)	$H_{\mathrm{hf},A}$ (kOe)	δ_A (mm/s)	$\Gamma_A^{1,6}$ (mm/s)	F_A (%)	$H_{\mathrm{hf},B}$ (kOe)	H_{dip} (kOe)	δ_B (mm/s)	$2\epsilon_{Q,B1}$ (mm/s)	$2\epsilon_{Q,B2}$ (mm/s)	$\Gamma_B^{1,6}$ (mm/s)	F_{B1} (%)	F_{B2} (%)
130	504	0.356	0.26	33	480		0.756	0.00		0.41	67	
135	503	0.352	0.27	35	479	−2.5	0.752	0.11	−0.12	0.35	33	33
160	502	0.357	0.29	35	475	−2.9	0.733	0.22	−0.07	0.35	16	50
260	494	0.296	0.25	35	464	−4.0	0.679	0.18	−0.05	0.29	17	49
300	489	0.273	0.25	35	457	−3.7	0.656	0.16	−0.05	0.28	16	48
400	475	0.211	0.25	36	439	−2.6	0.592	0.14	−0.04	0.27	16	48
486	454	0.156	0.29	36	413	−2.4	0.529	0.09	−0.02	0.32	16	48
588	422	0.088	0.31	37	378		0.452	0.01		0.33	63	
701	367	0.023	0.29	35	321		0.369	0.01		0.33	65	
814	255	−0.027	0.37	36	219		0.277	0.00		0.38	64	
837	198	−0.029	0.45	33	169		0.248	0.00		0.49	67	
854	146	−0.021	0.86	33	127		0.245	0.00		0.75	67	
873		−0.030	0.32	38			0.224	0.14		0.32	62	

doublet with quadrupole splitting $\Delta E_{Q,B} \approx 0.14$ mm/s, both having linewidths of 0.30 mm/s. Example fits are shown in Fig. 2. This finding is consistent with the local cubic symmetry on the A sites and the trigonal one on the B sites. A very similar line shape was observed earlier by Pan and Evans[41] for Fe_3O_4, but these authors fitted with a single line, claiming that a superposition of two or more components leads to physically unacceptable hyperfine data. In contrast, Becker and von Wurmb[42] resolved their paramagnetic Fe_3O_4 spectra into a singlet and a doublet, but are not specific about the parameters.

Table II compares the different compositions at $T = 125$ K, for which all samples have only one B-site component, and at 300 K. These data show that all six compositions have nearly identical Mössbauer parameters. One exception to that finding is the B-site linewidth which increases with increasing x, in contrast to the A-site width which is small and fairly constant. Table I further shows that, for a given x, $\Gamma_B^{1,6}$ increases with decreasing T much more rapidly as compared to $\Gamma_A^{1,6}$. Moreover, this differential broadening is enhanced by the Co substitution. For $x = 0.04$, e.g., it was found that $\Gamma_B^{1,6} = 0.37$ mm/s and $\Gamma_A^{1,6} = 0.31$ mm/s at 500 K, whereas $\Gamma_B^{1,6} = 0.75$ mm/s and $\Gamma_A^{1,6} = 0.29$ mm/s at 100 K. These seemingly minor effects are not artifacts and their importance will be discussed in detail in the next section.

The dipolar fields H_{dip} for all x values and at selected temperatures (140, 180 and 250 or 255 K), were also evaluated from the AFMS with $H_{\text{ext}} = 60$ or 55 kOe. An example spectrum is shown in Fig. 3 and refers to $x = 0.01$ at 255 K and in a 60-kOe field. Clearly, the $\Delta m_I = 0$ absorptions are absent meaning that the ferrimagnetically ordered A- and B-site spins are collinear with $\mathbf{H}_{\text{ext}}$, i.e., with the direction of propagation of the incident γ rays. Since the B-site magnetic moment is largest, it will go parallel to $\mathbf{H}_{\text{ext}}$. Hence, for the observed effective field H_{eff} in the AFMS, H_{ext} will subtract from $H_{\text{hf},B}$ and add to $H_{\text{hf},A}$. The B-site component, unlike the A-site one, is clearly asymmetric, the sixth line (lines 2 and 5 are absent, see Sec. III) being significantly deeper, and consequently sharper, than the first line. This feature was present in all the AFMS and was reproduced excellently by the aforementioned asymmetrical line profile (full line in Fig. 3).

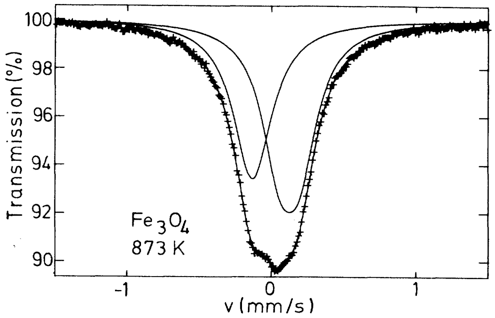

FIG. 2. Mössbauer spectrum of Fe_3O_4 above its Curie point. The spectrum is fitted with a singlet (A sites) and a doublet (B sites).

A selection of numerical results from the fits is presented in Table III. The hyperfine fields were obtained from the measured effective fields following $H_{\text{eff},A} = H_{\text{hf},A} + H_{\text{ext}}$ and $H_{\text{eff},B} = H_{\text{hf},B} - H_{\text{ext}}$. For comparison, the H_{hf} values obtained from the ZFMS, recorded under exactly the same conditions, but with the field switched off, are included as well. Both the sign and the magnitude of the dipolar fields are in agreement with the H_{dip} values derived from the ZFMS for $x = 0$, 0.005, and 0.01. Further, the A-site hyperfine fields evaluated from the AFMS and from the ZFMS are almost exactly the same.

TABLE II. Mössbauer parameters of the A- and B-site iron nuclei in the investigated $Co_xFe_{3-x}O_4$ spinels at 125 K (upper half) and at 300 K (lower half). For $x = 0$, 0.005, and 0.01 at 300 K, two B-site components can be resolved.

			A sites					B sites		
x	$H_{\text{hf},A}$ (kOe)	δ_A (mm/s)	$2\epsilon_{Q,A}$ (mm/s)	$\Gamma_A^{1,6}$ (mm/s)	F_A (%)	$H_{\text{hf},B}$ (kOe)	δ_B (mm/s)	$2\epsilon_{Q,B}$ (mm/s)	$\Gamma_B^{1,6}$ (mm/s)	F_B (%)
0	504	0.368	−0.00	0.30	35	480	0.762	0.00	0.44	65
0.005	506	0.362	−0.01	0.28	35	481	0.750	0.01	0.34	65
0.01	505	0.364	0.00	0.28	35	480	0.756	0.01	0.37	65
0.02	503	0.365	−0.01	0.27	37	480	0.762	0.00	0.44	64
0.03	505	0.359	−0.01	0.26	34	481	0.765	0.01	0.44	66
0.04	505	0.358	0.00	0.26	36	482	0.757	−0.01	0.57	64
0	489	0.273	−0.00	0.25	35	457	0.656	0.16	0.28	16
								−0.05		48
0.005	491	0.280	0.00	0.23	36	459	0.657	0.17	0.25	18
								−0.04		46
0.01	492	0.278	0.00	0.26	35	459	0.658	0.17	0.28	16
								−0.04		48
0.02	489	0.267	−0.00	0.26	36	458	0.656	0.00	0.32	64
0.03	490	0.269	0.01	0.26	36	459	0.654	0.00	0.32	64
0.04	489	0.260	−0.01	0.25	36	458	0.655	0.00	0.38	64

TABLE III. A selection of hyperfine-field values in kOe as obtained from the zero-field Mössbauer spectra H_{hf}(ZF), and from applied-field spectra H_{hf}(AF). The dipolar fields (B sites) obtained from the external-field runs are indicated as well.

	T		A sites		B sites		
x	(K)	H_{ext}	H_{hf}(ZF)	H_{hf}(AF)	H_{hf}(ZF)	H_{hf}(AF)	H_{dip}
0	255	60	494	494	464	471	−5
0.005	255	55	496	494	466	472	−3
0.01	255	60	496	495	467	473	−4
0.02	250	55	494	495	466	471	−4
0.03	250	55	496	495	467	471	−5

This means that the combined, external-field-induced demagnetizing and Lorentz field on the A sites, and hence on the B sites, is negligibly small. In contrast, there is a significant discrepancy between the ZFMS and AFMS hyperfine fields for the B sites. This cannot be due to an incorrect readout of the field strength since if that were true, then the A-site values should show an opposite effect. Therefore, it must be concluded that the external field triggers or inhibits some additional contribution to the B-site hyperfine field.

V. DISCUSSION

Prior to discussing the numerous hyperfine data, it should be stressed at this point that the stoichiometry of the various absorber materials has not been affected markedly by the annealing process. This conclusion is inferred from the fact that the VT temperatures, as observed from the Mössbauer spectra, exactly coincide with the values measured by magnetostriction on the original single crystals.[36] Since the VT is generally extremely sensitive to deviations from stoichiometry, it may be concluded that the stoichiometry of the involved samples has not been altered by the annealing. Also, the sharpness of the magnetic order-disorder transition supports this conclusion.

A. Linewidths

As mentioned in the previous section, the B-site lines broaden considerably on lowering the temperature, whereas the A-site lines remain sharp throughout the entire temperature range, except on reaching T_C where the Co substitution and the resulting chemical disorder create observable distributions on the magnetic exchange interactions and hence on the hyperfine fields.

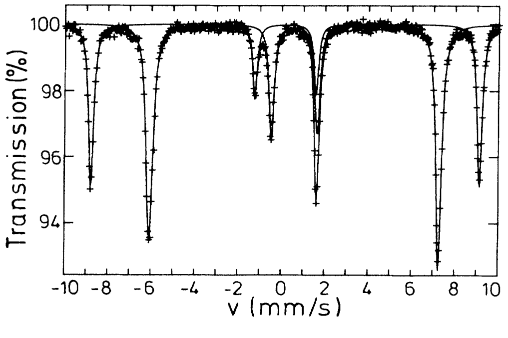

FIG. 3. Mössbauer spectrum of $Co_{0.01}Fe_{2.99}O_4$ at 255 K and in an external magnetic field of 60 kOe, clearly showing the absence of the $\Delta m_I = 0$ transitions.

The differential line broadening in Fe_3O_4 has been observed before by Sawatzky, Coey, and Morrish.[43] These authors related $\Delta W = \Gamma_B - \Gamma_A$ to the activation energy E_A of the electron exchange process and derived the expression

$$1/\Delta W = a_0 e^{-E_A/kT} , \tag{9}$$

with a_0 a constant and k Boltzmann's constant. When they plotted $\ln(\Delta W^{-1})$ vs T^{-1} they clearly observed two distinct linear regions with different slopes. For high temperatures ($T > 250$ K) they found $E_A = 0.065$ eV, whereas at low T the slope is very small. Without being specific, the authors suggested that at low T a different process takes place which affects the Mössbauer spectra but not the conductivity.

In the early 1970s, the idea of Sawatzky, Coey, and Morrish was abandoned and the B-site line broadening was exclusively attributed[24,44] to the aforementioned existence of two distinct components. Later experiments of van Diepen on a single-crystal Fe_3O_4 (Refs. 45 and 46) were said to confirm that conclusion. The present results, however, show that even after taking into account the two B-site subspectra, a considerable differential line broadening remains.

Figure 4 shows the $\ln(\Delta W^{-1})$ vs T^{-1} curves for some $Co_xFe_{3-x}O_4$ samples as obtained in the present study and referring to the widths of the outermost lines. They clearly confirm the earlier results of Sawatzky, Coey, and Morrish.[43] The E_A values for the low- and high-temperature processes, $E_{A,L}$ and $E_{A,H}$, respectively, derived from linear least-squares fitting are listed in Table IV, as well as a rough estimate of the temperature T_K which can be considered as quantifying the transition between the two exchange processes. The $E_{A,H}$ value for the present Fe_3O_4 is much smaller than that indicated by Sawatzky, Coey, and Morrish, however these authors fitted their spectra with a single B-site component, resulting in additional broadening for that component. The high-temperature behavior of the composition $x = 0.01$ is clearly not in line with that of the other compositions. It is believed that this is unreal, and probably due to some experimental instabilities in the course of the experiments

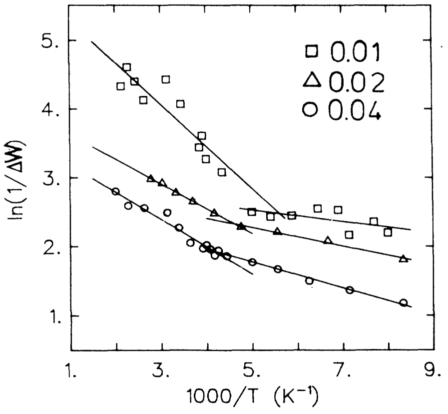

FIG. 4. Plot of the logarithm of the inverse differential line broadening $\Delta W = \Gamma_B - \Gamma_A$ vs the inverse temperature for three $Co_xFe_{3-x}O_4$ samples. Full lines are linear least-squares fits.

on that particular sample. One must bear in mind that at high T the values for ΔW are very small (0.05 mm/s or less) and that for $x = 0.01$ two B-site subspectra are required, leading to less accurate parameter values, and consequently a lot of scatter in the $\Delta W(T)$ variation.

The existence of two exchange mechanisms, as inferred by these Mössbauer results, seems to be consistent with the theoretical considerations of Ihle and Lorenz,[29] who predict a more bandlike process at low temperatures and a more localized hopping at high temperatures. The data in Table IV indicate that the high-T process is poorly affected by the Co substitution, at least for $x \leq 0.04$, whereas the activation energy of the low-T bandlike exchange increases with increasing x and more and more approaches the value of $E_{A,H}$, suggesting that for some x value between 0.04 and 0.1 the bandlike process is suppressed and only local hopping takes place. Amazingly, also the transition seems to shift upwards as the substitution increases.

The high value for $E_{A,L}$ of the Fe_3O_4 sample is consistent with its low value of T_V and again attributable to its lower stoichiometry. For ideal magnetite, Sherman[47] recently quoted the value $E_A = -0.016$ eV based on his molecular-orbital calculations aimed to explain the optically induced intervalence charge transfer in a number of minerals. This result is obviously in line with the data of Table IV. Also Goodenough[48] mentions the possibility of a negative activation energy for Fe_3O_4. The negative sign of the activation energy is due to the fact that any two neighboring B sites have almost exactly the same structural characteristics so that the sixth $3d$ electron has no preference for any of the two sites, and no energy is required to trigger the hopping. If, however, sufficient foreign ions or vacancies are introduced into the octahedral sublattice, an energy gap will be created and the activation energy becomes positive and further increases with increasing number of disturbing elements. It is unclear to the authors, however, why these departures from ideal stoichiometry would have a lesser effect on the more localized hopping process, unless collectiveness plays an important role in that respect.

TABLE IV. Activation energies for the high- and low-temperature electron-exchange processes, $E_{A,H}$ and $E_{A,L}$ respectively, as determined from the differential line broadening. T_K is a rough estimate of the border temperature between the two regions.

x	$E_{A,L}$ (eV)	$E_{A,H}$ (eV)	T_K (K)
0	0.017	0.036	280
0.005	−0.009	0.030	140
0.01	0.007	0.048	160
0.02	0.012	0.032	220
0.03	0.016	0.038	240
0.04	0.016	0.035	245

B. Center shifts

A typical variation of the center shift δ with temperature is shown in Fig. 5. The experimental $\delta(T)$ curve can be interpreted based on the well-known relation (see Ref. 49 and references therein)

$$\delta(T) = \delta_I + \delta_{\mathrm{SOD}}(T) , \tag{10}$$

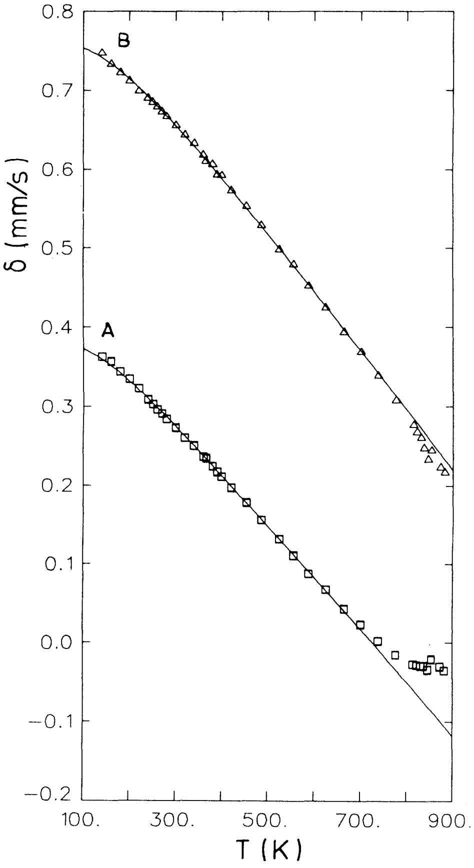

FIG. 5. Temperature variations of the A- and B-site center shifts δ for $Co_{0.01}Fe_{2.99}O_4$. Full lines are adjusted curves.

in which δ_I is the intrinsic isomer shift which is a measure for the *s*-electron density at the nucleus and commonly considered to be temperature independent. The second-order Doppler shift $\delta_{\mathrm{SOD}}(T)$, which results from the nonzero mean-square velocity of the nuclei, is usually expressed in terms of the Debye approximation for the lattice vibrations. As such, a parameter called the *characteristic Mössbauer temperature* Θ_M enters into the formula and can be evaluated by fitting that formula to the experimental data.

In a recent paper by one of the present authors,[49] it was reported that this procedure yielded very good reproductions of the experimental $\delta(T)$ curves measured for T values of up to ≈ 600 K for a wide variety of natural and synthetic Fe^{2+}-and/or Fe^{3+}-containing compounds, with consistent values for the adjusted Θ_M parameter. For higher temperatures, small deviations were observed due to a weak linear dependence of δ_I on T. This is also the case for the A-site center shifts of the present $Co_xFe_{3-x}O_4$ samples, at least if data for $T \geq 750$ K are not taken into account. An example fit is demonstrated by the full line in Fig. 5. The obtained $\Theta_{M,A}$ values range within 665 ± 25 K, which must be considered as an acceptable accuracy limit. The slopes $d\delta_I/dT$ were found to be of the order of -10^{-4} mm/(s K), and are comparable to those reported for other compounds.[49]

For the octahedral iron the above fitting procedure did not yield acceptable results and it is suggested that the electron-exchange process somehow causes an additional, higher-order temperature dependence of the electron density at the octahedral iron nuclei. Phenomenologically, a third-order one was found to yield acceptable results, with $\Theta_{M,B}$ values in the range 570 ± 15 K. Surprisingly, the presently found values for Θ_M, when averaged over A and B sites, are close to the reported Debye temperatures Θ_D for Fe_3O_4 as derived from specific heat measurements, i.e., 570 K (Ref. 50) and 660 K.[51]

The rather large difference between $\Theta_{M,A}$ and $\Theta_{M,B}$ for a given x might question the above interpretation of the $\delta(T)$ variations. To a large extent, Θ_M is positively correlated to the strength of the iron-oxygen bond, which is stronger on the tetrahedral sites due to the shorter bond length. Moreover, the B-site iron has a formal 2.5+ state and this lower charge as compared to A-site iron implies a weaker bond. Similar features have been found when comparing Θ_M values for Fe^{2+} and Fe^{3+} in structurally related compounds, the latter showing a Θ_M which is typically 100–150 K higher than that for the divalent iron.[49]

When the temperature reaches ≈ 750 K, the A-site center shifts suddenly start to decrease much more slowly with increasing T than one would expect from theory, an effect which is enhanced by the presence of Co. This is illustrated by Fig. 6 which shows the difference $D(T) = \delta_B - \delta_A$ as a function of T for those compositions for which the scans were extended to above T_C. It is seen from these drawings that the difference between the low-temperature saturation value, $D(100)$, and the value at some given high temperature, say $D(800)$, increases from ≈ 0.06 mm/s for $x = 0$ to ≈ 0.12 mm/s for $x = 0.03$. It should be mentioned at this point that these features are not artifacts from the fitting, as one might suggest considering the peculiar line shape of the spectra on approaching T_C. Indeed, several data points in the graphs of Fig. 5 refer to the paramagnetic state of the samples for which the spectra are much simpler.

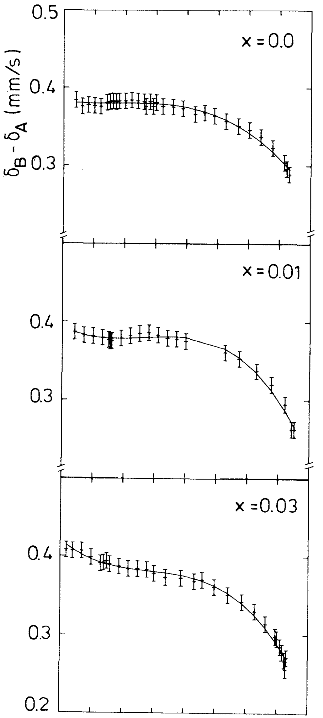

FIG. 6. Difference between the B- and A-site center shifts as a function of temperature for three $Co_xFe_{3-x}O_4$ samples. Full lines are meant as a guide for the eye.

Similar peculiarities in the high-temperature center shifts have been observed before by Pan and Evans[41] and by Håggström *et al.*[17] and were attributed to the A-site ferric ions becoming involved in the electron-exchange process at high temperatures in the vicinity of or exceeding T_C. If this interpretation is correct, then the present results would indicate that the presence of (a small amount of) Co on the B sites, which undoubtedly hinders the electron exchange between octahedral iron, instead enhances the exchange between A- and B-site iron.

C. Quadrupole interaction

For reasons mentioned in earlier sections, a detailed variation of the B-site quadrupole interaction $\Delta E_Q = e^2qQ/2$ in a broad temperature interval could only be obtained for the nonsubstituted sample and is depicted in Fig. 7. The data points near 900 K represent the quadrupole splittings obtained from the paramagnetic spectra for which the sign of the EFG cannot be determined. On the basis of the calculations presented hereaf-

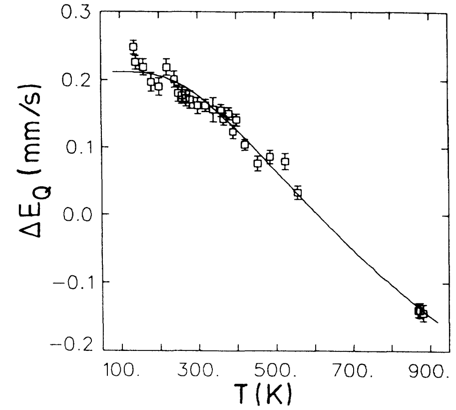

FIG. 7. Temperature variation of the quadrupole splitting for nonsubstituted magnetite. Full line is the adjusted curve based on the crystalline-field model for the electronic states of the ferrous ions (trigonal compression of the octahedral coordination).

ter, a negative sign was assumed. Since the data for ϵ_Q for $x=0.005$ in the range 215–385 K, and for $x=0.01$ in the range 230–500 K are the same within the experimental error limits to those for $x=0.0$, any significant dependence on x is unlikely.

Following the successful interpretation by Ding *et al.*[52] of the temperature variation of the quadrupole splitting for an (Fe^{2+},Fe^{3+}) dimer showing electron hopping, the observed *B*-site ΔE_Q for the present ferrites was considered as the time average of the Fe^{3+} and Fe^{2+} values, leading to the expression for the EFG's principal component *eq*,

$$eq = eq_{\text{lat}} + \tfrac{1}{2} eq_{\text{val}} , \tag{11}$$

with eq_{lat} the lattice contribution and eq_{val} the valence contribution of the ferrous state. Using the approximation of Ingalls[53] and assuming that eq_{lat} does not change with *T*, the temperature dependence of *eq* can be written as

$$eq(T) = eq_{\text{lat}} + \tfrac{1}{2} eq_{\text{val}}(0)\alpha^2 F(T) , \tag{12}$$

in which $eq_{\text{val}}(0)$ is the 0-K contribution of a 3*d* electron of the free-ion Fe^{2+} [≈ 3.7 mm/s (Ref. 54)] and α^2 the reduction due to covalency, which for spinel ferrites is between 0.6 and 0.9.[31] The function $F(T)$ contains the thermal populations of the electronic levels of the ferrous ions, and thus depends on the local symmetry.

Since in Fe_3O_4 the oxygen parameter *u* equals 0.379,[55] the octahedral coordination exhibits a trigonal compression and hence the ferrous ground state is expected to be an orbital singlet. The first excited state, with energy gap δ_t, is a doublet. Higher-energy states are not important since they are not occupied in normal laboratory conditions. Neglecting spin-orbit and spin-spin coupling, the full curve shown in Fig. 6 was adjusted to the data with parameters $\delta_t = 900\ \text{cm}^{-1}$, $eq_{\text{lat}} = -0.51$ mm/s, and $eq_{\text{val}}(0)\alpha^2 = 1.45$ mm/s.

Both δ_t and eq_{lat} have reasonable values,[31] however, the third parameter has the wrong sign and its magnitude would lead to an $\alpha^2 \approx 0.4$, which is believed to be unrealistic. Therefore, it is concluded that the *B*-site EFG and its temperature variation cannot be explained by a time average of 2+ and 3+ states in a trigonally compressed octahedron.

Similar calculations assuming a doublet ground state yielded more acceptable results, with correct sign and proper magnitude of the 0-K valence term and with approximately the same values for δ_t and eq_{lat}, except for the sign of the latter one. The covalency reduction was found to be 0.8.

A doublet ground state for the Fe^{2+} state in Fe_3O_4 seems to be questionable. For most known spinel systems containing Fe^{2+} on the octahedral sites and with localized 3*d* electrons, the magnetocrystalline anisotropy constants are correctly predicted by models assuming an orbital singlet for the ferrous ground state.[56] This is not the case for Fe_3O_4,[57] which has tentatively been ascribed to the electron-exchange process. Kronmüller and Walz[58] have argued that, due to local distortions associated with the electron hopping, at least part of the ferrous ions in magnetite could have a doublet ground state. To the best of the authors' knowledge, the electronic properties of magnetite and substituted magnetites remain puzzling to date.

D. Magnetic hyperfine interactions

The reduced hyperfine fields $h(T) = H_{\text{hf}}(T)/H_{\text{hf}}(0)$, when plotted against the reduced temperature T/T_C for the six different compositions all follow the same curve for both *A* and *B* sites, and any significant dependence on the Co concentration could not be observed, except for the Curie temperature which slightly decreases with increasing *x*. This correlation will be discussed in the second part of this study. Also, the reduced sublattice magnetizations $m_{S,A}$ and $m_{S,B}$ for Fe_3O_4, as determined from neutron diffraction,[40] show the same temperature variation as compared to the corresponding reduced fields, meaning that to a very good approximation the relation $h(T) = m_S(T)$ is valid for both lattice sites.

It is common to describe $H_{\text{hf}}(T)$ in spinel ferrites using the Heisenberg model for the sublattice magnetizations. In the simple case that iron is the only magnetic ion on both sublattices *A* and *B*, the hyperfine fields $H_{\text{hf},A}(T)$ and $H_{\text{hf},B}(T)$ may be written as

$$H_{\text{hf},A}(T) = H_{\text{hf},A}(0) B_S\{(5/2kT)[2z_{AA}J_{AA}\langle S_{z,A}(T)\rangle - 2z_{AB}J_{AB}\langle S_{z,B}(T)\rangle]\} , \tag{13}$$

$$H_{\text{hf},B}(T) = H_{\text{hf},B}(0) B_S\{(5/2kT)[-2z_{BA}J_{AB}\langle S_{z,A}(T)\rangle + 2z_{BB}J_{BB}\langle S_{z,B}(T)\rangle]\} , \tag{14}$$

in which $B_S(X)$ is the Brillouin function for spin S,

$$B_S(X)=\frac{2S+1}{2S}\coth\left[\frac{2S+1}{2S}X\right]-\frac{1}{2S}\coth\left[\frac{X}{2S}\right] . \qquad (15)$$

The quantities z_{ij} in expressions (13) and (14) are the number of magnetic j-site nearest neighbors to an i-site iron, and J_{ij} the corresponding exchange integral which is positive for a ferromagnetic interaction; $\langle S_{z,i}(T)\rangle$ is the expectation value of the z component of the i-site spin at temperature T. Since the latter is proportional to $m_i(T)$, i.e., to $H_{\mathrm{hf},i}(T)$, the hyperfine fields at any given T can be solved iteratively from (13) and (14) for any given set of J_{ij} values, which may thus be evaluated by least-square fitting to the experimental field values.

That fitting procedure was applied for the samples $x=0.0$, 0.01, and 0.03, yielding for the exchange integrals $J_{AA}=-11$ K, $J_{AB}=-22$ K, and $J_{BB}=3$ K. The positive sign of the latter one is consistent with the well-known, ferromagnetic Zener double exchange in systems with electron exchange.[59] The values found for the A-A and A-B interactions are in line with those for iron-iron interactions in several other spinel ferrites[31] as determined from the variation of the hyperfine fields. In spite of these consistencies, the fit must be termed unsuccessful since it describes the experimental curves rather poorly. Many attempts have been made to modify the basic model, introducing, e.g., temperature-dependent exchange integrals, an adjustable B-site spin value, and a supertransferred hyperfine-field contribution.[31] To some extent the fit could be improved, but it could never be considered acceptable.

It was reasonable at that point to presume that the electron-exchange process on the B sites is responsible for the inadequacy of the Heisenberg model to reproduce the temperature variation of the hyperfine fields in magnetite and substituted magnetites. This was proved to be correct by calculating $H_{\mathrm{hf},A}(T)$ from (13) using the experimentally obtained reduced B-site hyperfine fields as expectation values of the reduced B-site spin. In that way $H_{\mathrm{hf},A}(T)$ was reproduced very precisely with $J_{AA}=-11$ K, $J_{AB}=-23$ K, and $T_C=870$ K. The same procedure carried out for $H_{\mathrm{hf},B}(T)$, again yielded unacceptable results.

A fairly good description of $H_{\mathrm{hf},B}(T)$ was obtained using the non-localized-electron model (NLEM) developed by Kubo and Ohata[60] to explain the spontaneous magnetization of Ca^{2+}-substituted $\mathrm{LaMnO_3}$ perovskite which shows electron hopping between Mn^{3+} and Mn^{4+}. These authors represented the magnetic ions by localized spins with magnitude S_l. The nonlocalized electrons were assumed to belong to a given energy band with mean bandwidth $\gamma_S(X)$ and $X=g\mu_B SH_m/kT$, H_m being the molecular field. Without going into the details, the relevant expressions can be summarized as follows:

$$h(T)=m_S(T)=B_S(X) , \qquad (16)$$

in which S is the localized spin plus the electron spin, i.e., $S_l+\frac{1}{2}$. This means that the nonlocalized electrons are assumed to be strongly coupled to the localized spins to form resultant spins with $S_l+\frac{1}{2}$. The argument X in (16) is determined by

$$\frac{T}{T_C}X=\frac{15S(2S+1)}{(2S-1)(4S+1)}\,\frac{d\gamma_S(X)/dX}{dm_S(X)/dX}\equiv F_S(X) , \qquad (17)$$

in which the bandwidth γ_S is given by

$$\gamma_S(X)=\frac{S}{2S+1}\left[\frac{2S+1}{2S}+\coth\left[\frac{2S+1}{2S}X\right]\times\left[\coth X-\frac{1}{2S}\coth\frac{X}{2S}\right]\right] . \qquad (18)$$

Given values to the parameter set $[T_C, H_{\mathrm{hf},B}(0), S]$, X can be calculated iteratively from the expressions (17) and (18) at any given temperature, and the parameters can thus be determined by fitting to the experimental field data. Figure 8 is an example fit, referring to $\mathrm{Fe_3O_4}$ and showing the excellent agreement between observed and calculated B-site hyperfine fields. The parameters were found to be $T_C=875$ K, $H_{\mathrm{hf},B}(0)=480$ kOe, and $S=2.9$. The latter figures were also obtained for $x=0.01$ and 0.03, whereas $T_C=870$ K and 850 K, respectively, all in reasonable agreement with the earlier mentioned values for the Curie temperature. Finally, the bandwidth γ_S at room temperature was calculated to be 0.82 eV, which is remarkably close to Sherman's result of 0.84 eV,[47] as obtained from his interpretation of the optical spectra of magnetite. Such a broad bandwidth corresponds to a temperature of the order of 10^4 K, which is much higher than the trigonal field splitting. This feature might explain why the common crystalline-field model cannot be applied to interpret the temperature variation of the EFG

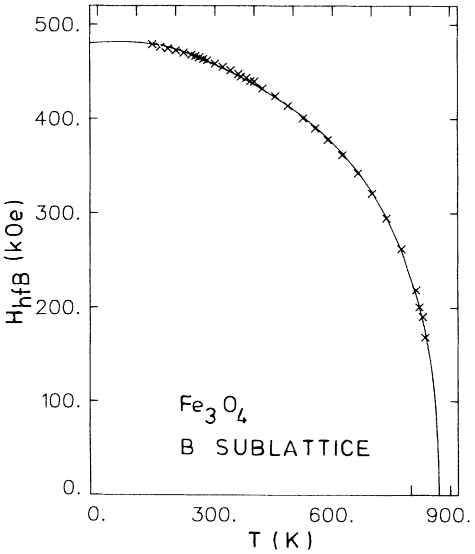

FIG. 8. Temperature behavior of the B-site hyperfine field $H_{\mathrm{hf},B}$ for $\mathrm{Fe_3O_4}$. The full line is the calculated dependence based on the non-localized-electron model of Kubo and Ohata.

in these magnetites.

In conclusion, using the NLEM, the temperature variation of the B-site hyperfine field in Fe_3O_4 for the first time could be reproduced adequately, yielding reasonable values for the involved physical quantities.

E. Dipolar field

The temperature variations of the dipolar field H_{dip} for $x=0$, 0.005, and 0.01 are shown in Fig. 9. The minus sign indicates that it is opposite to the Fermi-contact field. Due to the relatively large errors, it cannot be concluded if the presence of Co has any effect on the value of H_{dip} and/or on its relation with T. Håggström *et al.*[17] reported a much higher magnitude for H_{dip} in Fe_3O_4, i.e., ≈ 10 kOe and not depending on T. However, it was found by the present authors that their high value is an artifact resulting from their assumption that all 18 absorption lines have the same linewidth, which in view of these results is undoubtedly not justified. A higher value for $|H_{dip}|$ was also reported by Boekema,[38] however this author did not specify how his spectra had been decomposed.

From the well-known relation between H_{dip} and the EFG's principal component, eq, i.e., $H_{dip}=-\mu_B eq$,[61] a 0-K dipolar term of -5 kOe is calculated ($e^2qQ/2=0.2$ mm/s and $Q=0.21\times 10^{-28}$ m^2). Further, from the splitting of the B-site resonance line in the NMR experiments of Rubinstein, Strauss, and Bruni[62] on Fe_3O_4, one calculates a value of 5.6 kOe for the magnitude of the dipolar field at RT, which is in reasonable agreement with the present results.

According to Boekema,[38] the temperature variation of the dipolar field on the B sites in magnetite is given by

$$H_{dip}(T)=\left[H_{dip}^{lat}+H_{dip}^{val}\frac{1-e^{-\delta_t/kT}}{1+2e^{-\delta_t/kT}}\right]\frac{S_z(T)}{S_0} . \tag{19}$$

The term within brackets is similar to expression (12) for the quadrupole splitting, assuming a singlet ground state for the ferrous ions, and has the same physical background. The additional term $S_z(T)/S_0$ describes the temperature dependence of the reduced net magnetic moment.

Boekema claimed that his experimental $|H_{dip}(T)|$ values for magnetite show a maximum at around 200 K and related this finding to the minimum in the cubic anisotropy constant K_1 as reported by Chikazumi.[63] Adjusting expression (19), using calculated values for the lattice and valence contributions, the author found $\delta_t=100$ K, which is unrealistically low.

As for the present study, the relatively large scatter of the obtained H_{dip} values does not allow us to conclude whether or not there is a minimum in the range 200–300 K. The full lines in Fig. 9 are the calculated variations based on expression (19), the trigonal splitting δ_t, and the valence term H_{dip}^{val} being adjustable parameters. Again it was assumed that the electronic state of the B-site iron is the average of pure Fe^{3+} and Fe^{2+} states. The lattice contribution was estimated to be 22 kOe (same sign as the Fermi-contact hyperfine field) from lattice summation over one unit cell and is in good agreement with the value quoted by Boekema.[38] The reduced net magnetic moment at each temperature was determined from the reduced hyperfine field at that temperature. In this way, the zero-Kelvin valence dipolar fields for the pure Fe^{2+} states were found to be -52 kOe for both $x=0$ and $x=0.005$ and -50 kOe for $x=0.01$. The trigonal splittings were 1400, 1000, and 1000 cm^{-1}, respectively, which are reasonable values. The valence contributions, however, are much smaller than those which are typically found for Fe^{2+} in trigonal crystalline fields, i.e., between -200 and -300 kOe depending on δ_t.[62,64] It is believed that the small magnitude of the valence dipolar fields in the investigated magnetites might somehow be related to the broad bandwidth, as found from the NLEM. The exact nature of the effect, however, is not clear, and as mentioned before, the same effect might as well be responsible for the failure of the crystalline-field model to explain the valence contribution to the ferrous EFG.

F. Effect of applied fields

As mentioned in Sec. IV, there is a significant discrepancy between the B-site hyperfine field values observed from the zero-field spectra and those determined from the effective field $H_{eff,B}$ derived from the applied-field spectra. This is illustrated in Fig. 10 in which the sum $H=H_{eff,B}+H_{ext}$ is plotted against H_{ext} for three $Co_xFe_{3-x}O_4$ samples. In each case, that sum should be constant and equal to the corresponding hyperfine field $H_{hf,B}$. Instead, H increases with increasing external-field

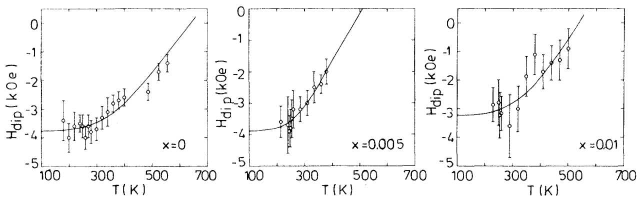

FIG. 9. B-site dipolar fields for three $Co_xFe_{3-x}O_4$ samples. Full lines are calculated dependences.

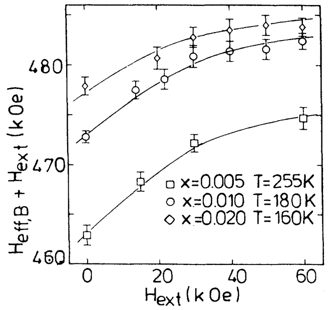

FIG. 10. Sum $H=H_{eff,B}+H_{ext}$ as a function of the external field H_{ext} for three $Co_xFe_{3-x}O_4$ samples, showing the appearance of a field-induced contribution to the total hyperfine field at the octahedral iron nuclei.

strength, possibly reaching saturation at H_{ext} values higher than those available to the authors. As for the A-site components, the difference $H_{\mathrm{eff},A}-H_{\mathrm{ext}}$ remains equal to $H_{\mathrm{hf},A}$ within experimental error limits.

The behavior of H as depicted in Fig. 10 indicates the presence of an additional field contribution, opposite to the Fermi-contact field and induced by the external field. It is conceivable to relate this effect to the nonlocalized $3d$ electrons and one could think of some kind of polarization process of the spins of these electrons. However, this suggestion is rather tentative at present and a more systematic study using variable temperatures and external-field strengths, preferably exceeding 60 kOe, is required in order to form a more detailed picture of this observed phenomenon.

VI. CONCLUSION

It is clear that the electronic and magnetic properties of the investigated cobaltous magnetites with small substitution degree are predominantly dictated by the fast electron exchange between the octahedral ferrous and ferric ions. According to the B-site linewidths, the nature of this exchange process at low temperatures above the Verwey transition is different from that at relatively high temperatures, say above RT. This finding seems to be consistent with the suggestion of Ihle and Lorenz[29] that in Fe_3O_4 below RT a band-conduction mechanism is dominant, whereas at higher temperatures a small-polaron hopping conduction becomes the essential mechanism. If this picture is correct, then it can additionally be concluded from the present results that the presence of Co suppresses the band mechanism and that only the more locally confined hopping process is expected to take place in the entire temperature range if the fraction x of cobalt ions exceeds a certain threshold value between 0.04 and 0.1.

For the first time, the temperature dependence of the B-site hyperfine field in magnetite could be reproduced adequately. This was achieved by modifying the band model developed by Kubo and Ohata[60] for the electron hopping between Mn^{3+} and Mn^{4+} in certain perovskites. The bandwidth was calculated to be 0.82 eV and is not significantly affected by the Co concentration up to $x=0.03$. The broad energy band is believed to be the reason for the shortcoming of the crystalline-field model to describe the temperature variation of the electric-field gradient and of the dipolar field at the octahedral iron nuclei, representing the electronic state of the irons as time-averaged divalent and trivalent states.

Also the B-site center shift is strongly affected by the exchange process. Additional terms in the temperature dependence of the intrinsic isomer shifts are required in order to explain the variation with T of the observed shift with reasonable values for the involved physical quantities. As for the A-site ferric ions, the drastic discrepancy between experimental and calculated center shifts at temperatures in the vicinity of and above T_C suggests that at high temperatures the A sites become involved in the exchange of electrons.

Finally, from applied-field measurements it is concluded that an additional contribution to the total effective B-site field is induced by the external field. Its appearance is tentatively explained by polarization of the nonlocalized electrons.

ACKNOWLEDGMENTS

The authors wish to thank Dr. V. A. M. Brabers (Techn. Univ., Eindhoven) for kindly providing the single crystals. They are thankful to Dr. D. Gryffroy and Mr. A. Van Alboom for helpful and stimulating discussions. This research was supported by the Fund for Joint Basic Research, Belgium (Grant No. 20055.87) and by the National Fund for Scientific Research, Belgium (Research Grant No. 31567289).

---

*Present address: Research Group Materials, (Vlaams Instituut voor Technologisch Onderzock), B-2400 Mol, Belgium.

[1] E. J. W. Verwey and F. de Boer, Recl. Trav. Chim. Pays Bas **55**, 531 (1936).
[2] E. J. W. Verwey and P. W. Haayman, Physica **8**, 979 (1941).
[3] S. Iida, K. Mizushima, H. Mizoguchi, J. Mada, S. Umemura, K. Nakoo, and J. Yoshida, in *Magnetism and Magnetic Materials—1975 (Philadelphia),* Proceedings of the 21st Annual Conference on Magnetism and Magnetic Materials, edited by J. J. Becker, G. H. Lander, and J. J. Rhyne, AIP Conf. Proc. No. 29 (AIP, New York, 1976), p. 388.
[4] M. A. Gilleo, Phys. Rev. **109**, 777 (1958).
[5] R. Bauminger, S. G. Cohen, A. Marinov, S. Ofer, and E. Segal, Phys. Rev. **122**, 1447 (1961).
[6] J. L. Dormann, C. Djega-Mariadassou, and V. A. M. Brabers, in *Proceedings of the International Conference on the Application of the Mössbauer Effect,* edited by V. G. Bhide (Indian National Science Academy, New Delhi, 1982), pp. 196–198.
[7] R. M. Persoons, Ph.D. thesis, University of Gent, 1990.
[8] K. Ono, Y. Ishikawa, A. Ito, and E. Hirahara, J. Phys. Soc. Jpn. **17**, Suppl. B-1, 125 (1962).
[9] S. K. Banerjee, W. O. Reilly, and C. E. Johnson, J. Appl. Phys. **38**, 1289 (1967).
[10] B. J. Evans and S. S. Hafner, J. Appl. Phys. **40**, 1411 (1969).
[11] J. M. Daniels and A. Rosencwaig, J. Phys. Chem. Solids **30**, 1561 (1969).
[12] W. Kündig and R. S. Hargrove, Solid State Commun. **7**, 223 (1969).
[13] D. C. Dobson, J. W. Linnett, and M. M. Rahman, J. Phys. Chem. Solids **31**, 2727 (1970).
[14] J. M. D. Coey, A. H. Morrish, and G. A. Sawatzky, J. Phys. (Paris) Colloq. **32**, C1-271 (1971).
[15] C. Boekema, J. De Jong, F. van der Woude, and G. A. Sawatzky, Physica **86-88B**, 948 (1977).
[16] B. J. Evans and G. Amthauer, Phys. Chem. Minerals **3**, 66 (1978).
[17] L. Häggström, H. Annersten, T. Ericsson, R. Wäppling, W. Karner, and S. Bjarman, Hyperfine Interact. **5**, 201 (1978).
[18] G. Amthauer, *High-Pressure Researches in Geoscience* (E. Schweizerbart'sche Verlagsbuchhandlung, Stuttgart, 1982),

pp. 269–292.

[19] B. J. Evans and Lu-San Pan, J. Appl. Phys. **61**, 4352 (1987).

[20] B. J. Evans, in *Magnetism and Magnetic Materials—1972 (Denver),* Proceedings of the 18th Annual Conference on Magnetism and Magnetic Materials, edited by C. D. Graham and J. J. Rhyne, AIP Conf. Proc. No. 10 (AIP, New York, 1972), p. 1398.

[21] H. N. Ok and B. J. Evans, Phys. Rev. B **14**, 2956 (1976).

[22] B. J. Evans and H. N. Ok, Physica **86-88B**, 931 (1977).

[23] J. W. Linnett and M. M. Rahman, J. Phys. Chem. Solids **33**, 1456 (1972).

[24] C. I. Nistor, C. Boekema, F. van der Woude, and G. A. Sawatzky, in *Proceedings of the 5th International Conference on Mössbauer Spectroscopy, Bratislava, Czechoslovakia, 1973,* edited by M. Muel and T. Zemcik (Czechoslovak Atomic Energy Commission, 1975), pp. 96–113.

[25] P. J. Murray and J. W. Linnett, J. Phys. Chem. Solids **37**, 619 (1976).

[26] C. Boekema, F. van der Woude, and G. A. Sawatzky, J. Phys. C **9**, 2439 (1976).

[27] J. L. Dormann, T. Merceron, P. Renaudin, and V. A. M. Brabers, J. Phys. (Paris) Colloq. **41**, C1-177 (1980).

[28] M. Bhaduri, J. Chem. Phys. **77**, 1400 (1982).

[29] D. Ihle and B. Lorenz, J. Phys. C **18**, L647 (1985).

[30] L. R. Bickford, J. Pappis, and J. L. Stull, Phys. Rev. **99**, 1210 (1955).

[31] R. E. Vandenberghe, E. De Grave, in *Mössbauer Spectroscopy Applied to Inorganic Chemistry,* edited by G. J. Long and F. Grandjean (Plenum, New York, 1989), Vol. 3, pp. 59–182.

[32] R. Leyman, PhD thesis, Gent State University, 1987.

[33] G. Le Caër and J. M. Dubois, J. Phys. E **12**, 1083 (1979).

[34] S. J. Campbell and F. Aubertin, in *Mössbauer Spectroscopy Applied to Inorganic Chemistry* (Ref. 34), Vol. 3, pp. 183–242.

[35] E. De Grave, R. Leyman, and R. Vanleerberghe, Phys. Lett. **97A**, 354 (1983).

[36] R. M. Persoons and E. De Grave, Solid State Commun. **72**, 977 (1989).

[37] R. M. Persoons, E. De Grave, and R. E. Vandenberghe, Hyperfine Interact. **54**, 655 (1990).

[38] C. Boekema, Ph.D. thesis, Groningen State University, 1977.

[39] B. J. Evans, in *Magnetism and Magnetic Materials—1974 (San Francisco),* Proceedings of the 20th Annual Conference on Magnetism and Magnetic Materials, edited by C. D. Graham, G. H. Lander, and J. J. Rhyne, AIP Conf. Proc. No. 24 (AIP, New York, 1975) p. 73.

[40] T. Riste and L. Tenzer, J. Phys. Chem. Solids **19**, 117 (1961).

[41] L. S. Pan and B. J. Evans, in *Magnetism and Magnetic Materials—1976 (Pittsburgh),* Proceedings of the First Joint MMM-Intermag Conference, edited by J. J. Becker and G. H. Lander, AIP Conf. Proc. No. 34 (AIP, New York, 1976) p. 181.

[42] K. D. Becker and V. von Wurmb, Z. Phys. Chem. **149**, S77 (1986).

[43] G. A. Sawatzky, J. M. D. Coey, and A. H. Morrish, J. Appl. Phys. **40**, 747 (1969).

[44] B. J. Evans, in *Magnetism and Magnetic Materials—1971 (Chicago),* Proceedings of the 17th Annual Conference on Magnetism and Magnetic Materials, edited by D. C. Graham and J. J. Rhyne, AIP Conf. Proc. No. 5 (AIP, New York, 1971), p. 296.

[45] A. M. van Diepen, Phys. Lett. **57A**, 354 (1976).

[46] A. M. van Diepen, Physica **86-88B**, 955 (1977).

[47] D. M. Sherman, Phys. Chem. Minerals **14**, 355 (1987).

[48] J. B. Goodenough, in *Mixed-Valence Compounds,* edited by D. B. Brown (Reidel, Dordrecht, 1980), pp. 413–425.

[49] E. De Grave and A. Van Alboom, Phys. Chem. Minerals **18**, 337 (1991).

[50] R. W. Millar, J. Am. Chem. Soc. **51**, 215 (1929).

[51] J. S. Kouvel, Phys. Rev. **102**, 1489 (1956).

[52] X. Q. Ding, E. L. Bominaar, E. Bill, H. Winkler, and A. X. Trautwein, J. Chem. Phys. **28**, 178 (1990).

[53] R. Ingalls, Phys. Rev. **128**, 1155 (1962).

[54] A. Vermaas, W. Groeneveld, and J. Reedijk, Z. Naturforsch. Teil A **37**, 1393 (1977).

[55] S. C. Abrahams and B. A. Calhoun, Acta Crystallogr. **6**, 105 (1953).

[56] J. C. Slonczewski, J. Appl. Phys. Suppl. **32**, S253 (1961).

[57] J. Smit, F. K. Lotgering, and R. P. Van Stapele, J. Phys. Soc. Jpn. **17**, 268 (1962).

[58] H. Kronmüller and F. Walz, Philos. Mag. B **42**, 433 (1980).

[59] C. Zener, Phys. Rev. **82**, 403 (1951).

[60] K. Kubo and N. Ohata, J. Phys. Soc. Jpn. **33**, 21 (1972).

[61] F. van der Woude, Phys. Status Solidi **17**, 417 (1966).

[62] M. Rubinstein, G. H. Strauss, and F. J. Bruni, in *Particles and Fields—1977 (Argonne),* Proceedings of the 1977 Meeting of the APS Division of Particles and Fields, edited by P. A. Schreiner, G. H. Thomas, and A. B. Wicklund, AIP Conf. Proc. No. 43 (AIP, New York, 1972), p. 1384.

[63] S. Chikazumi, in *Magnetism and Magnetic Materials—1975 (Philadelphia),* Proceedings of the 21st Annual Conference on Magnetism and Magnetic Materials, edited by J. J. Becker, G. H. Lander, and J. J. Rhyne, AIP Conf. Proc. No. 29 (AIP, New York, 1972), p. 382.

[64] F. Hartmann-Boutron and P. Imbert, J. Appl. Phys. **39**, 775 (1968).